Bioconjugate Chemistry

Article

pubs.acs.org/bc

Conjugation of Basic Fibroblast Growth Factor on a Heparin Gradient for Regulating the Migration of Different Types of Cells

Jindan Wu,[†,‡] Zhengwei Mao,[†] Yifeng Hong,[†] Lulu Han,[†] and Changyou Gao*[,†,§]

[†]MOE Key Laboratory of Macromolecular Synthesis and Functionalization, Department of Polymer Science and Engineering, Zhejiang University, Hangzhou 310027, China

[‡]MOE Key Laboratory of Advanced Textile Materials & Manufacturing Technology, College of Materials and Textile, Zhejiang Sci-Tech University, Hangzhou 310018, China

[§]State Key Laboratory of Diagnosis and Treatment for Infectious Diseases, First Affiliated Hospital, College of Medicine, Zhejiang University, Hangzhou 310003, China

Supporting Information

ABSTRACT: Regulation of cell migration by cell growth factors is critical in tissue regeneration such as angiogenesis, wound healing, and bone formation. In this work, basic fibroblast growth factor (bFGF) with a density varying between 0 and 295 ng/cm^2 was conjugated on heparinized glass slides. The amount of conjugated bFGF was determined by immunofluorescent staining. The mobility of vascular smooth muscle cells (VSMCs) was largely dominated by the bFGF density, whereas that of mesenchymal stem cells (MSCs) and endothelial cells (ECs) was slightly influenced. The migration rate of VSMCs increased initially and then decreased along with the increase of bFGF density. The fastest rate (~22 μm/h) was found on the bFGF surface with a density of 83 ng/cm^2. The intrinsic mechanisms of the diverse migration behaviors of the VSMCs, MSCs, and ECs were revealed by studying the expression of bFGF receptors and migration-related proteins. The results show that the cell mobility is regulated by complex and synergetic intracellular signals in a cell type-dependent manner.

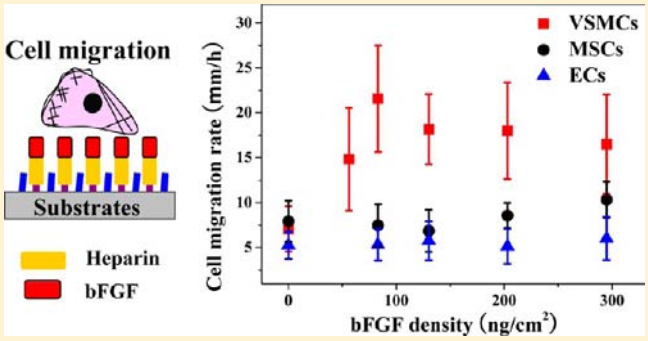

Regenerative medicine and tissue engineering aims to reconstruct living tissues for replacement of damaged or lost tissues/organs of living organisms.[1] For this context, cells are required to attach, migrate, proliferate, and differentiate on biomaterials that are often loaded with biosignaling molecules.[2−4] The interfacial relationships between biomaterials and cells strongly influence the success of biological processes during the tissue repair and regeneration, and thereby should be carefully elucidated.[5]

During this process, one of the key aspects is cell migration.[6] In mammals, cell migration plays a prominent role in physiological processes. For example, when a wound occurs, neutrophils arrives at the wound site within minutes and provide pro-inflammatory cytokines to attract fibroblasts and keratinocytes to invade into the temporarily formed clots.[7] Afterward, the epidermal cells proliferate and migrate to cover the surface.[8] The programmed process is controlled by the interplay of biosignals. Also, cell migration is important during tissue engineering. To achieve the regeneration of tissues or organs using biomaterials *in situ*, cells should be recruited from the nearby sites and undergo proliferation and differentiation in the specific microenvironment.[6] Thus, it is of paramount importance to correlate the cell migration behaviors with the surface properties of materials, so that the intrinsic mechanism and in turn biomaterial design can be fulfilled.

Many surface properties, especially the surface chemistry, are important for regulating cell migration. In a previous study, we demonstrated that the surface density of poly(ethylene glycol) (PEG) brushes dominate cell migration in a biphasic pattern.[9] The migration rates of vascular smooth muscle cells (VSMCs) are slower when the surface density of PEG brushes is too low or too high, while it reaches maximum values at a moderate density due to the proper adhesion force between cells and substrates. Many other bioactive molecules have been introduced onto surfaces to modulate cell migration too. For example, Mann et al. investigated the effects of surface-immobilized cell adhesion peptides (Arg-Gly-Asp (RGD), Lys-Gln-Ala-Gly-Asp-Val (KQAGDV), and Val-Ala-Pro-Gly (VAPG)) on the migration behaviors of VSMCs.[10] The cells migrate faster on surfaces with a peptide density of 0.2 nmol/cm^2, but slower on surfaces with a peptide density of 2.0 nmol/cm^2. Wacker et al. and Guarnieri et al. found that cells prefer to migrate to the areas with higher RGD densities.[11,12] Proteins such as fibronectin and vitronectin have also been found to accelerate cell migration.[13] Moreover, the cell migration rate can be increased by patterning

Received: December 16, 2012
Revised: June 5, 2013
Published: July 22, 2013

these proteins in a gradient formation. For example, Smith et al. reported that bovine aortic endothelial cells migrate faster on a fibronectin gradient with a larger slope in the range of 0.34 to 1.23 ng Fn/mm^3.[14,15] Cai et al. cultured endothelial cells on a collagen gradient surface and found that endothelial cells on the areas with low and moderate collagen surface densities display a stronger motility tendency in parallel to the gradient. By contrast, the cells growing on the gradient area with a high collagen density show a reverse response to the collagen gradient, suggesting that the cell motility is regulated by the collagen gradient with a surface-density dependent manner.[16]

Among all the molecules adopted to control the cell migration, the cell growth factors are regarded as promising candidates because they play important roles in tissue regeneration. For example, basic fibroblast growth factor (bFGF) is a paradigm of a group of nine closely related, multifunctional proteins known as fibroblast growth factor family (FGFs). The FGFs are heparin-binding proteins. Their interactions with cell-surface-associated heparan sulfate proteoglycans have been shown to be essential for FGF signal transduction. Although the cells are usually thought to react to soluble FGFs through their receptors on cell membrane, most of the FGFs present in extracellular matrix are in an immobilized state *in vivo*. FGFs induce proliferation, mitosis, migration, differentiation, and other various biological responses in most mesoderm and neuroectoderm-derived cells.[17−19] Owing to their powerful bioactivity, the FGFs are being used to treat surgical, burn, and periodontal tissue wounds, gastric ulcers, segmental bony defects, and ligament and spinal cord injury.[20] Kawai et al. reported that incorporation of bFGF in artificial dermis accelerates fibroblast proliferation and capillary formation in a dose-dependent manner.[21] Katsuno et al. demonstrated that released bFGF can promote the rapid completion of pancreaticojejunostomy anastomosis and improve the healing quality of granulation tissue by accelerating angiogenesis.[22]

Although the bFGF has been successfully used in tissue regeneration, much less attention is paid to elucidate their influence on cell migration especially after immobilization on substrates.[23−25] One of the main obstacles is maintenance of the activity of cell growth factors which generally have short half-life (less than 50 min).[26] For example, DeLong et al. prepared a hydrogel with a continuous bFGF density gradient by photopolymerization, which inevitably denatures a part of them.[24] Heparin, an anionic polysaccharide, can effectively bind and immobilize FGFs to enhance their stability.[27,28] Heparin and bFGF can form a complex even at an ultralow concentration (~pmol/L). Both the lifetime and the bioactivity of bFGF are enhanced in the complex. Taking this bioconjugation effect into consideration, in this work surfaces with different densities of heparin are first prepared, and then used to conjugate bFGF with variable densities.

In this study, influence of the surface-anchored bFGF on the migration behaviors of VSMCs, endothelial cells (ECs), and mesenchymal stem cells (MSCs) are investigated *in vitro*. These cells are essential in regeneration of tissues or organs, in particular, for angiogenesis. However, up to the present most of the migration results are based on the qualitative measurement. Herein, the cell motility as a function of the surface-conjugated growth factor density is quantitatively studied. The inherent mechanism is revealed by studying the expression levels of fibroblast growth factor receptors (FGFR) and some specific migration-related proteins.

MATERIALS AND METHODS

Materials and Regents. Basic fibroblast growth factor (bFGF, Mn ~ 18.5 kD) was purchased from the Center of Biotechnology Research and Development, Jinan University, Guangzhou, China. Heparin sodium (Mn ~ 26 kD) was purchased from Sinopharm Chemical Reagent Co., Ltd. *N*-Ethyl-*N*′-(3-dimethylaminopropyl) carbodiimide hydrochloride (EDC) and *N*-hydroxysuccinimide (NHS) were purchased from Aladdin Reagent Company. 3-Triethoxysilylpropylamin (APS) and 3-(trimethoxysilyl)propyl methacrylate (TMSPMA) were purchased from J&K company. All other chemicals were of analytical grade and used without further treatment if not otherwise stated. The water was purified by a Milli-Q water system (Millipore, USA).

Cell Culture. Human vascular smooth muscle cells (VSMCs) and endothelial cells (ECs) were obtained from the Cell Bank of Typical Culture Collection of Chinese Academy of Sciences (Shanghai, China). The VSMCs and ECs were maintained with regular growth medium consisting of high-glucose DMEM and RPMI 1640 (Gibco, USA), respectively, which were supplemented with 10% fetal bovine serum (FBS, Sijiqin Inc., Hangzhou, China), 100 U/mL penicillin, and 100 μg/mL streptomycin, and cultured at 37 °C in a 5% CO_2 humidified environment.

Mesenchymal stem cells (MSCs) were isolated from bone marrow of young adult male Sprague−Dawley rats as described previously.[29] The procedures were performed in accordance with the 'Guidelines for Animal Experimentation' by the Institutional Animal Care and Use Committee, Zhejiang University. Briefly, MSCs were obtained from the femoral shafts of rats by flushing out with 10 mL of culture medium (low glucose DMEM supplemented with 10% FBS, 100 U/mL penicillin, and 100 μg/mL streptomycin). The isolated cells were collected in two flasks (75 cm^2 culture flask, Corning Inc., USA) containing 15 mL culture medium and incubated in a humidified atmosphere of 95% air and 5% CO_2 at 37 °C. After reaching about 80% confluence, the cells were detached and serially subcultured. MSCs at passage 2 were used in this study.

Surface Preparation. Glass or silicon slides were cut into 1 × 1 cm^2 pieces and were consecutively cleaned in toluene, acetone, and alcohol under ultrasonication. They were further incubated in a "piranha" solution (a mixture of 30% hydrogen peroxide and 70% sulfuric acid (v/v)), thoroughly washed with

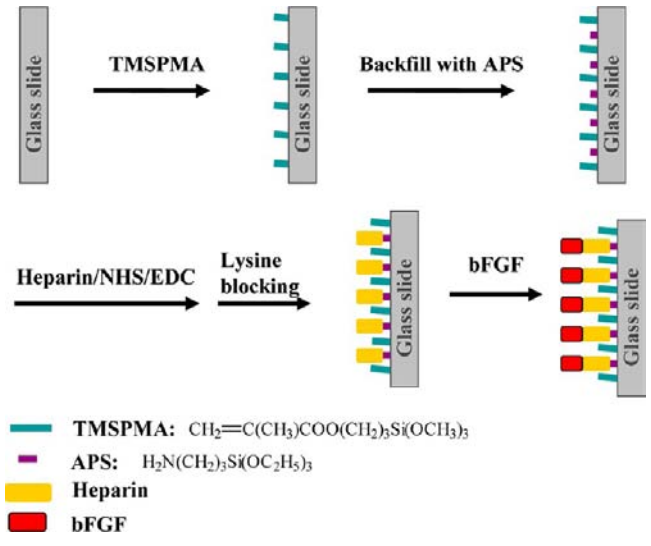

Figure 1. Schematic illustration to show the surface conjugation of bFGF via covalently immobilized heparin with a controlled density.

dx.doi.org/10.1021/bc300670t | *Bioconjugate Chem.* 2013, 24, 1302−1313

Table 1. N/C and the C−O/C−C Ratios of Silanized and Heparinized Surfaces Detected by XPS

sample	N/C	C−O−C/C−C
TMSPMA	/	0.33
Heparin+TMSPMA(30 min)	0.053	0.71
Heparin+TMSPMA(20 min)	0.065	0.78
Heparin+TMSPMA(5 min)	0.089	1.22
Heparin+TMSPMA(3 min)	0.109	1.58
Heparin+TMSPMA(0 min)	0.118	1.64

water, and dried under a nitrogen flow. The silanized surfaces were prepared according to the procedures described previously.[9] Briefly, the slides were first immersed into TMSPMA toluene solution (25 ng/mL) for a given period of time at room temperature. After washing with toluene 5 times, the slides were reacted with APS (25 ng/mL in toluene solution) for 30 min at room temperature. The slides were then thoroughly washed in toluene under ultrasonication, dried under a nitrogen flow, and finally baked at 50 °C for 4 h.

The silanized slides were immersed in 1 mg/mL heparin solution containing 5 mg/mL EDC and 5 mg/mL NHS for 4 h at 37 °C (the amount of heparin is excessive for the reaction to enable full coverage of the surface). After washing 5 times in water on a shaker to remove the physically adsorbed heparin

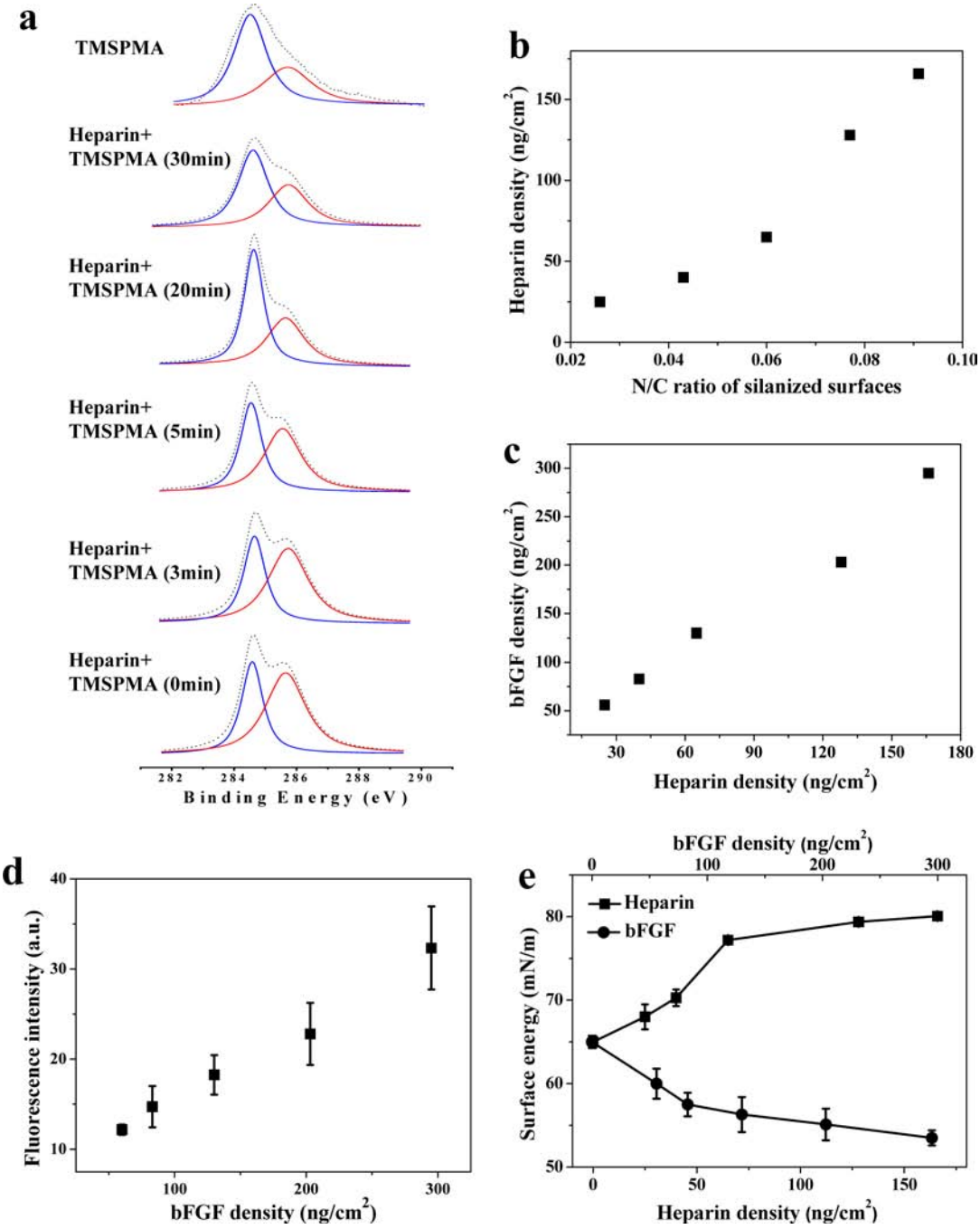

Figure 2. (a) XPS results of C1s peaks on heparin+TMSPMA/APS surfaces with different TMSPMA reaction time as noted in the figure. (b) Heparin density as a function of N/C ratio on silanized surfaces. (c) bFGF density as a function of heparin density on heparinized surfaces. (d) Relative fluorescence intensity of the surfaces as a function of bFGF density. (e) Surface energy as a function of heparin and bFGF densities, respectively.

dx.doi.org/10.1021/bc300670t | *Bioconjugate Chem.* 2013, 24, 1302−1313

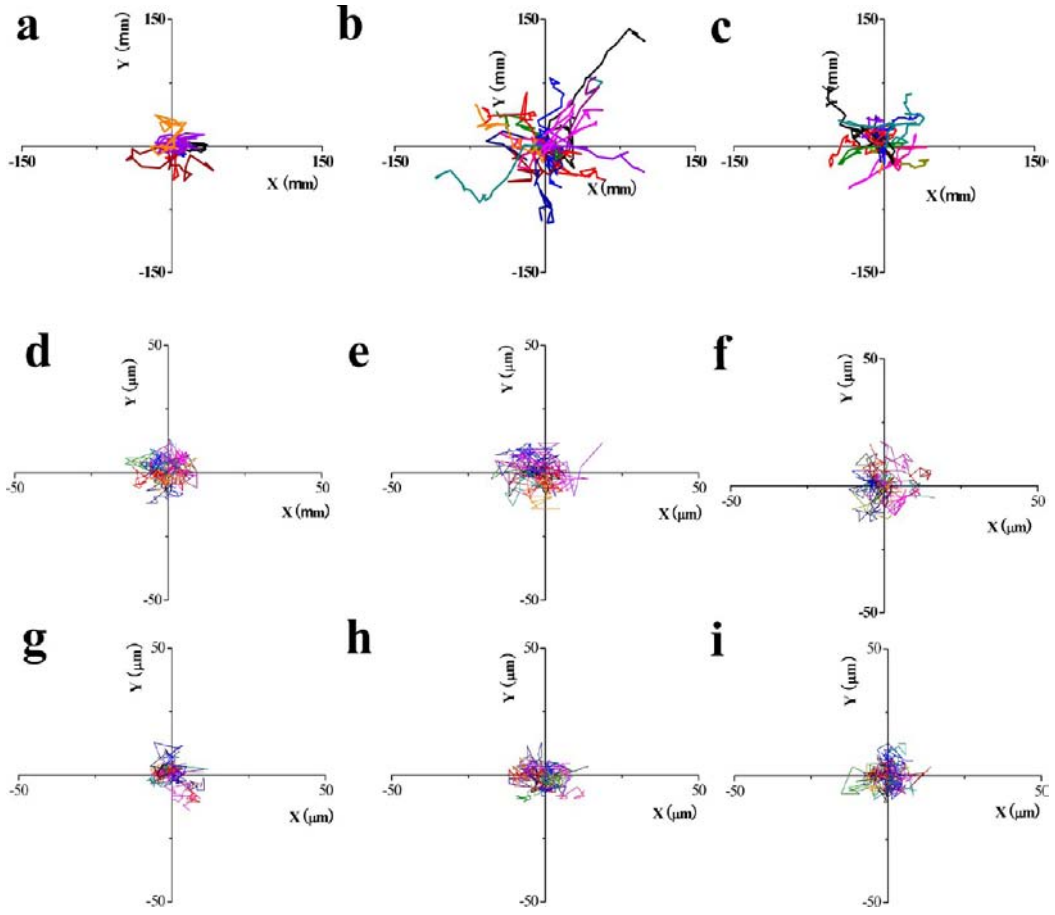

Figure 3. Migration traces of (a–c) VSMCs, (d–f) MSCs, and (g–i) ECs on surfaces of bFGF with a density of (a, d, g) 0 ng/cm^2, (b, e, h) 83 ng/cm^2, and (c, f, i) 295 ng/cm^2. Cells (n > 40) were continuously tracked every 30 min for 12 h (20 traces were randomly chosen to draw this figure). Their initial positions at the start are defined as the 0 point in the X–Y plane.

molecules, the slides were treated with 5 mg/mL lysine solution for 1 h at 37 °C to block the remaining reactive groups.

The heparinized slides were sterilized in 75% ethanol for 1 h, followed with 6 washings in phosphate buffered saline (PBS, pH 7.4), and then were immersed into 5 μg/mL bFGF PBS solution containing 0.1% BSA under aseptic condition for 1 h at room temperature. Finally, the substrates were gently washed with PBS 5 times and used immediately.

Surface Characterization. The chemical compositions of the surfaces were detected by an X-ray photoelectron spectrometer (XPS, Axis Ultra from Kratos Analytical, UK) with a monochromated Al Kα source at pass energies of 160 eV for survey spectra and 80 eV for core level spectra. Data were analyzed with the Kratos Vision Processing and XPS Peak software. The binding energy was corrected by setting the lowest binding energy of C 1s peak at 284.6 eV.

The surface grafting processes of heparin and bFGF were quantitatively monitored by quartz crystal microbalance with dissipation (QCM-D, Q-sense E4). The mass was calculated according to the change of resonance frequency. The quartz crystals with a 50 nm silica layer on the outmost surface were first cleaned by 1:1:5 mixture of ammonia, hydrogen peroxide, and water for 1 h and further silanized as described previously. Then the crystals were mounted into the reaction cells, into which the heparin/EDC/NHS solution was slowly injected at a rate of 50 μL/min. The reaction was maintained at 37 °C for 4 h. Finally, a large amount of water was injected into the

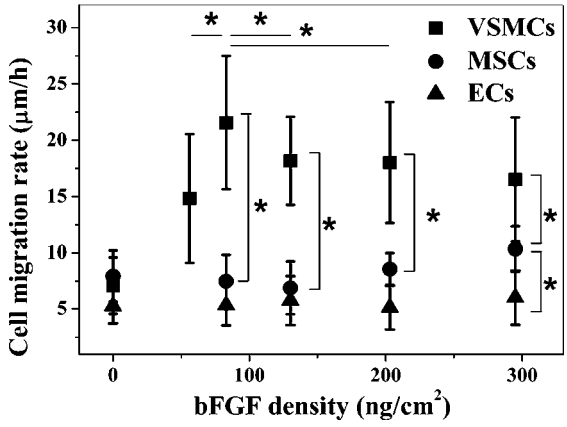

Figure 4. Migration rates of VSMCs, MSCs, and ECs as a function of bFGF density. The positions of the cells were continuously tracked every 30 min for 12 h. * indicates significant difference at p < 0.05.

reaction cells to wash away the unreacted heparin molecules. Five mg/mL lysine solution was injected into the cells and reacted for 1 h and then the reaction cells were thoroughly washed with water and PBS in sequence. Five μg/mL bFGF/PBS solution was then injected into the cells, maintained for 1 h, and plenty of PBS was injected into the cells to thoroughly remove the unconjugated bFGF molecules. The increased mass was calculated from frequency change using a Sauerbrey model with Q-tools software.

dx.doi.org/10.1021/bc300670t | Bioconjugate Chem. 2013, 24, 1302–1313

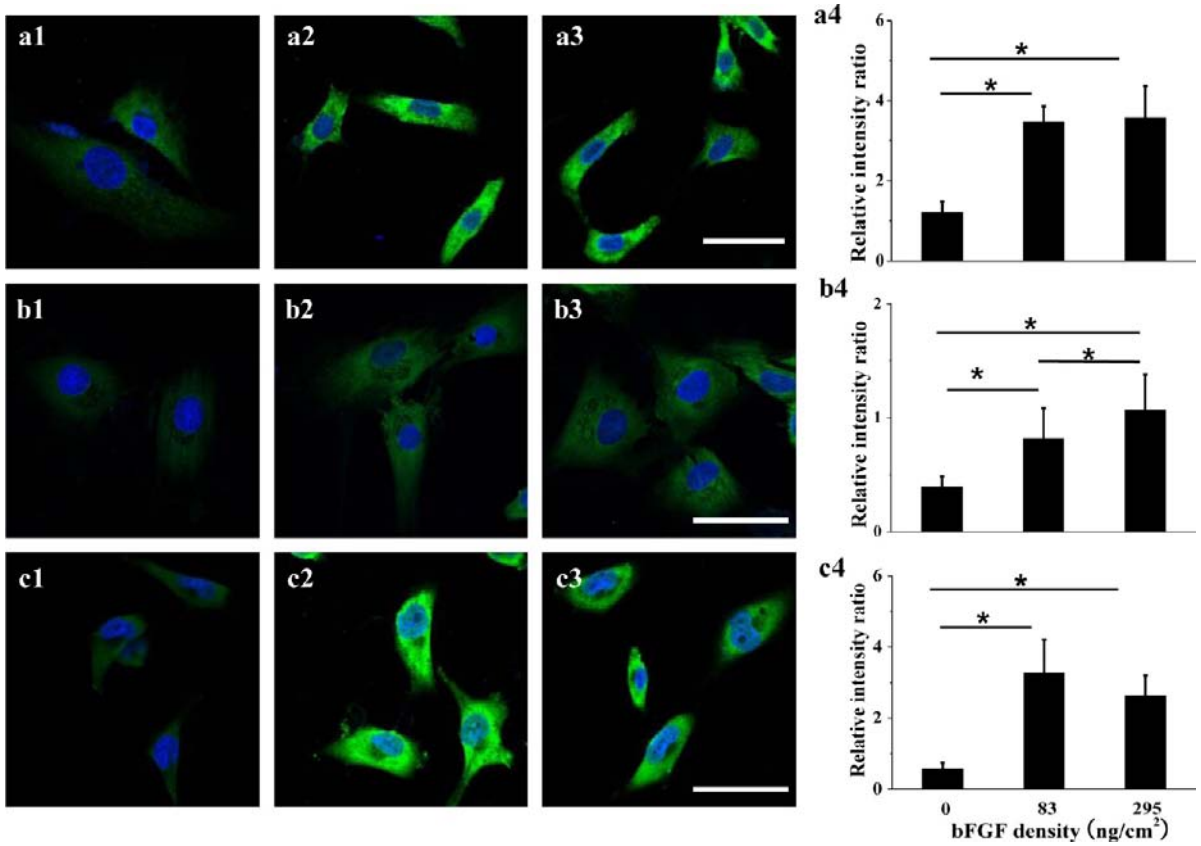

Figure 5. CLSM images of bFGFR of (a) VSMCs, (b) MSCs, and (c) ECs cultured for 24 h on surfaces of bFGF with a density of (1) 0 ng/cm^2, (2) 83 ng/cm^2, and (3) 295 ng/cm^2, respectively. bFGFR and cell nucleus were stained by the monoclonal antibody (green) and DAPI (blue), respectively. The scale bar is 50 μm. (4) Fluorescence intensity ratio of bFGFR calculated from (1) to (3) by IPP software as a function of bFGF density (relative to glass surface), respectively. * indicates significant difference at $p < 0.05$.

Immunochemistry was adopted to quantitatively characterize the surface-tethered bFGF. The slides with bFGF were first blocked in 1% BSA/PBS solution for 1 h, and then were treated with a rabbit monoclonal antibody against human recombinant bFGF (Beyotime, China) for 1 h at 37 °C. After washing 3 times with PBS, the slides were incubated with fluorescein isothiocyanate (FITC)-labeled goat anti-rabbit IgG (Beyotime, China) for 1.5 h at room temperature, followed by 5 washings in PBS. The slides were observed under fluorescence microscopy (IX81, Olympus) and their relative fluorescence intensity was analyzed by ImageJ software.

The static contact angles of water and diiodomethane were measured by a sessile-drop method on a DSA 100 contact angle measuring system (Krüss, Germany). The volume of each solvent droplet was 2 μL. The results were averaged from 5 independent measurements. Surface energy was calculated based on these data using an Owens-Wendt-Rabel-Kaelble method.

Cell Migration. The cells were seeded onto different surfaces at a density of 5×10^3 cells/cm^2 in order to minimize the influence of cell−cell interactions. Approximately 8 h post cell plating in 0.4% FBS DMEM, the cell migration behaviors were *in situ* recorded using a time-lapse phase-contrast microscope (IX81, Olympus) equipped with an incubation chamber (37 °C and 5% CO_2 humidified atmosphere) over a period of 12 h. Here the low concentration of FBS was used to minimize the potential influences of functional proteins in serum.

The cell trajectories were reconstructed from the center positions of individual cells over the whole observation time. The cell migration distance S was calculated by an Image pro Plus software according to the following equation at 0.5 h time intervals over the observation time of 12 h ($t = 12$).

$$S = \sum_{i=1}^{t} \sqrt{(x_i - x_{i-1})^2 + (y_i - y_{i-1})^2} \quad (1)$$

At least forty cells were calculated for each sample. The cell migration rates (ν) are thus obtained by $\nu = S/t$.

Cellular Expression of FGF Receptor (FGFR) and Migration-Related Proteins. Staining of bFGFR and migration-related proteins Cdc 42, Myosin IIA, Rac1, and RhoA was performed. Briefly, after the cells were cultured in the medium containing 0.4% FBS for 24 h, they were carefully washed with PBS 3 times, and then were fixed with 4% paraformaldehyde at 37 °C for 30 min, followed by 3 washings in PBS. The cells were further treated in 0.5% (v/v) Triton X-100/PBS at 4 °C for 10 min to enhance the permeability of the cell membrane. After rinsing 3 times with PBS, they were incubated in 1% BSA/PBS at 37 °C for 30 min to block the nonspecific interactions. The samples were first incubated with a monoclonal antibody against bFGFR, Cdc 42, Myosin IIA, Rac1, and RhoA (Abcam), respectively. After washing twice in 1% BSA/PBS, they were incubated with corresponding FITC-labeled IgG (Beyotime, China) and DAPI for 1 h at room temperature. After thoroughly washing against PBS, the cells were observed under a fluorescent microscope (CLSM, SP 5, Leica) and the relative fluorescence intensity was analyzed by an IPP software. At least twenty cells were measured for each protein expression.

dx.doi.org/10.1021/bc300670t | *Bioconjugate Chem.* 2013, 24, 1302−1313

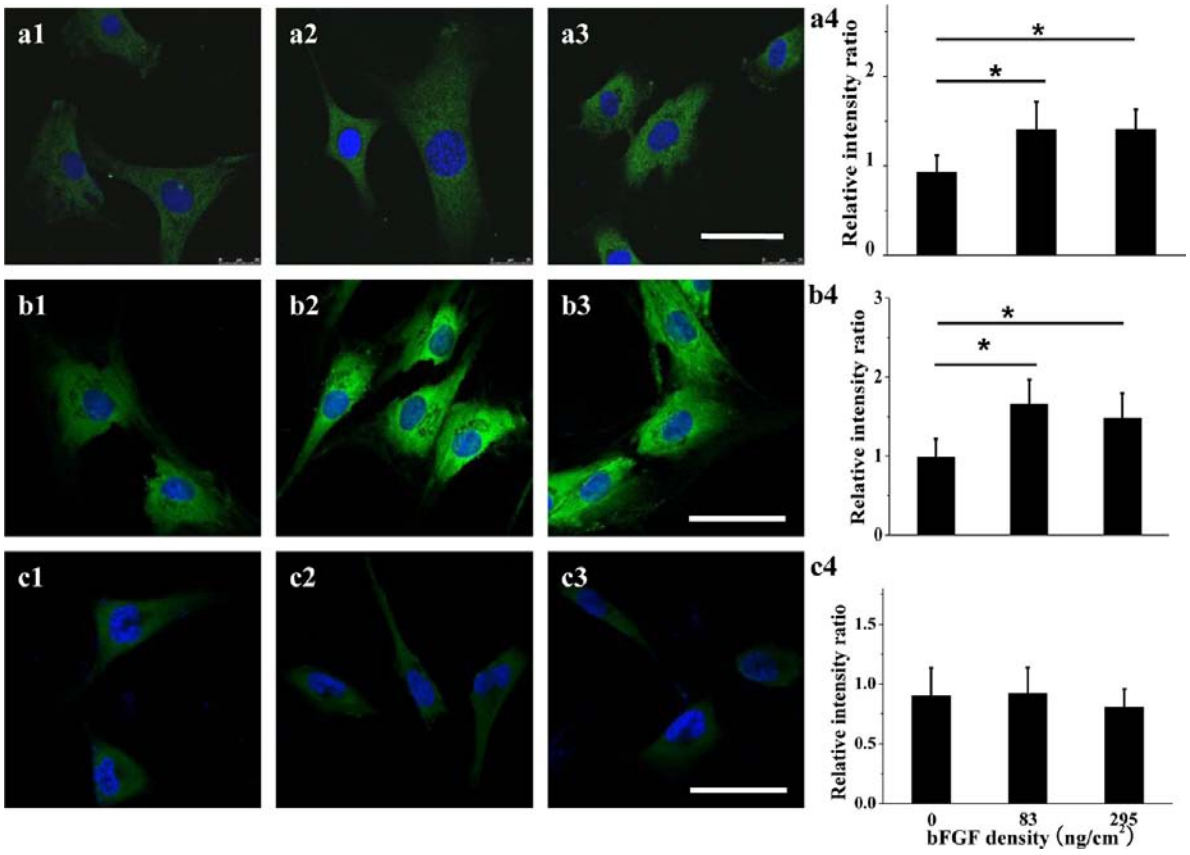

Figure 6. CLSM images of Cdc42 of (a) VSMCs, (b) MSCs, and (c) ECs cultured for 24 h on surfaces of bFGF with a density of (1) 0 ng/cm^2, (2) 83 ng/cm^2, and (3) 295 ng/cm^2, respectively. Cdc42 and cell nucleus were stained by the monoclonal antibody (green) and DAPI, respectively. The scale bar is 50 μm. (4) Fluorescence intensity ratio of Cdc42 calculated from (1) to (3) by IPP software as a function of bFGF density (relative to glass surface), respectively. * indicates significant difference at $p < 0.05$.

Statistic Analysis. The data are expressed as mean ± standard deviation (SD). The statistical significance between groups is determined by one-way analysis of variance (ANOVA) in the Origin software. The Tukey Means Comparison method is performed and the statistical significance is set as $p < 0.05$.

RESULTS AND DISCUSSION

Preparation and Characterization of Heparin and bFGF Surfaces. The preparation method and processes of surface-grafted heparin and bFGF brushes are illustrated in Figure 1. As reported previously, the density of amino groups on the silanized surfaces could be adjusted by controlling the reaction time of TMSPMA,[9] which can then determine the grafting density of heparin brushes via an EDC/NHS coupling reaction. Consequently, the density of bFGF is controlled due to the specific bioconjugation effect between heparin and bFGF, enabling good control over both the quality of samples in different batches and the maintenance of natural activity of the growth factor. It is worth mentioning that the introduced ethylene groups render the possibility of immobilizing other functional molecules by methods such as Michael addition. However, this will not be the focus of the present study.

XPS detection found that the atomic ratio of nitrogen to carbon (N/C ratio), which is proportional to the relative content of $-NH_2$ groups, increased when the reaction time of TMSPMA decreased, implying the variation of $-NH_2$ densities.[9] After grafting of heparin, the N/C ratio was further increased (Table 1) compared to the respective silanized surface, suggesting the successful immobilization of heparin (the N/C ratio in heparin is ∼0.11). Further evidence is provided by analysis of the ether groups (C−O−C bonds with C1s peak at 286 eV in XPS spectra) which exist exclusively in the heparin molecule (Figure 2a). The ratio of C−O−C/C−C (C1s peak at 284.6 eV) reflects the relative content of heparin on the surface. Table 1 shows that this ratio increased along with the decrease of TMSPMA reaction time, suggesting the stepwise adjustment of the density of heparin brushes.

The mass of heparin was further quantified by QCM-D. As shown in Figure 2b, the density of heparin increased almost linearly along with the N/C ratio on the silanized surfaces, which is in good accordance of the XPS results.

The structure of bFGF is a β trefoil fold which consists of four-stranded β sheets. The basic amino acid residues in the loop between β strands 10 and 11 form the interaction sites to heparin.[30,31] Thus, heparin binds to bFGF with a high degree of specificity and keeps the bioactivity of bFGF.[32] The conjugating process of bFGF was also monitored by QCM-D. The bFGF density linearly increased along with the heparin density, with a mass ratio of ∼1.6 between bFGF and heparin (Figure 2c). Considering the molecular weights, the molecular ratio between bFGF and heparin was calculated to be 2.2. Lam et al.[32] suggested a model complex between heparin and bFGF, and indicated that a heparin molecule bridges to two monomeric bFGF molecules based on the high stability and specific orientation of the dimeric complex. The ratio of bFGF and heparin obtained from QCM-D was very close to this value, lending

dx.doi.org/10.1021/bc300670t | Bioconjugate Chem. 2013, 24, 1302−1313

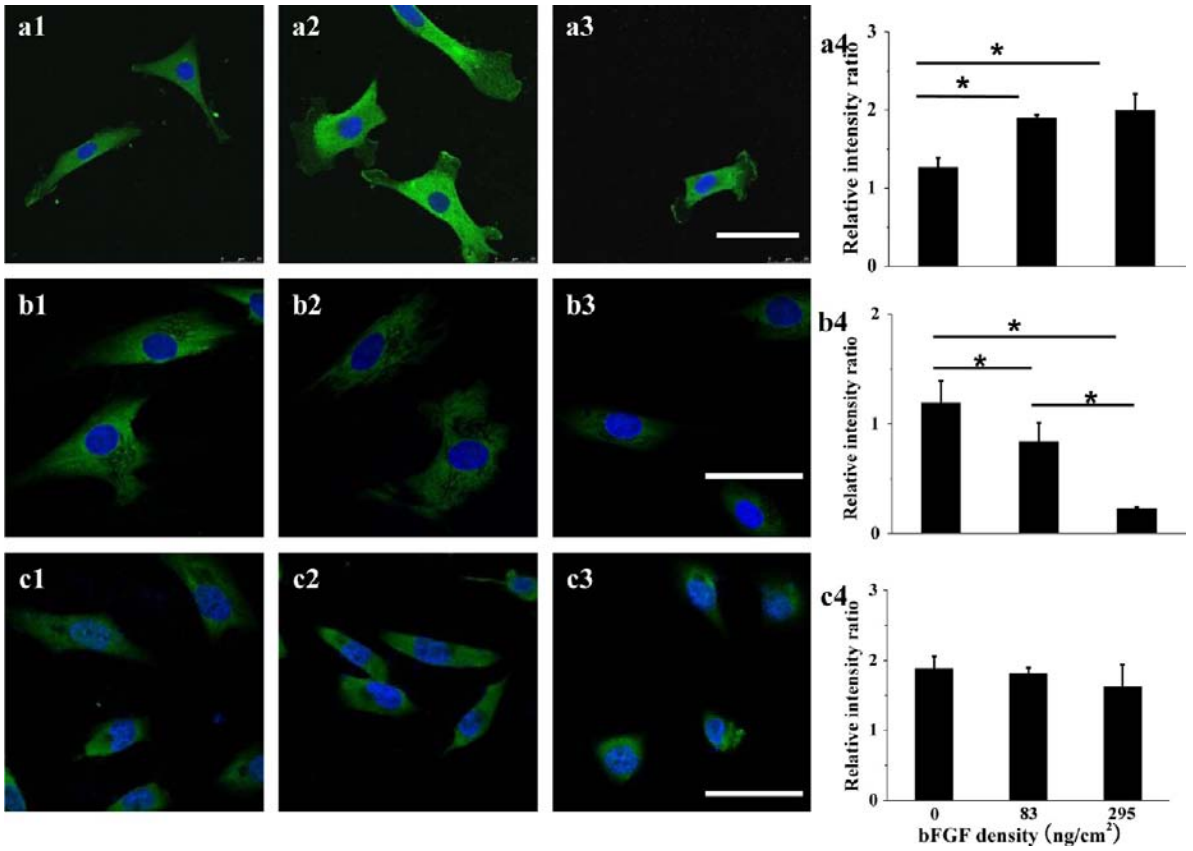

Figure 7. CLSM images of Rac1 in (a) VSMCs, (b) MSCs, and (c) ECs cultured for 24 h on surfaces of bFGF with a density of (1) 0 ng/cm^2, (2) 83 ng/cm^2, and (3) 295 ng/cm^2, respectively. Rac1 and cell nucleus were stained by the monoclonal antibody (green) and DAPI (blue). respectively. The scale bar is 50 μm. (4) Fluorescence intensity ratio of Rac1 calculated from (1) to (3) by IPP software as a function of bFGF density (relative to glass surface), respectively. * indicates significant difference at $p < 0.05$.

support to the bFGF–heparin binding model suggested by Lam et al.[32]

Some technologies have been developed to prolong the half-life of growth factors when they are introduced onto the matrix. Conjugation with heparin or hexuronyl hexosaminoglygan sulfate (HHS-4) is helpful for sustaining the biological activity of bFGF molecules.[33] Besides, dextran sulfate also can protect bFGF from inactivation.[34] In the present work, the relative amount of bFGF was analyzed by an immunofluorescence technology (Figure 2d). As shown in Figure 2d, the fluorescence intensity increased linearly along with the bFGF density, indicating the successful preparation of surfaces with tunable density of immobilized bFGF. Although the presence of antibody binding domain does not necessarily lead to the bioactivity of the bFGF, it somehow provides evidence that the structure of bFGF is largely retained after surface immobilization, which is highly related to the protein functions.

The surface energy of heparin and bFGF surfaces was calculated based on the results of water and diiodine methane contact angles (Figure 2e). The surface energy rapidly increased from 65 to 77 mN/m along with the increase of heparin density before 65 ng/cm^2 and then leveled off, revealing the sufficient coverage of hydrophilic heparin molecules. By contrast, the surface energy gradually decreased to 54 mN/m along with the increase of density of relatively hydrophobic bFGF. This alteration in wettability further supports the observation using other characterization techniques.

Cell Migration. bFGF is widely incorporated into biomaterials to accelerate tissue regeneration, such as angiogenesis,[35] osteogenesis,[36] and wound healing.[37] However, no attempt has been carried out to evaluate their influence on cell migration quantitatively, let alone the intrinsic mechanism.

ECs constitute the inner layer of blood vessel, and VSMCs are the main component of the media layer.[38] The migration of ECs and VSMCs is important during the regeneration of many tissues including blood vessel, wound healing, and myocardium. On the other hand, MSCs are cells originated from bone marrow and are frequently used in tissue regeneration due to their potential to differentiate into a variety of cell types. Indeed, MSCs can largely promote tissue regeneration, e.g., angiogenesis *in vivo* and *in vitro*.[39] Therefore, the mobility of these three types of cells on the bFGF surfaces was investigated.

In order to avoid cell–cell interactions, the cells were seeded at a low density. In this case, the mobility of cells is influenced by the cell–substrate interactions, which are determined by the bFGF density and the type of cells. The cells were monitored *in vitro* for 12 h and their representative migration trajectories on the bFGF surfaces were obtained (Figure 3). The three kinds of cells migrated randomly on all the surfaces without a preferable direction. This is reasonable since the cells would not directionally polarize in a uniform environment without directional chemical and/or physical cues. Compared with the VSMCs, the ECs and MSCs only migrated a shorter distance on the surfaces of the same bFGF density (Figure 3d–i). Moreover, on the TMSPMA surface (Figure 3a) and the surface with the highest bFGF density (Figure 3c), the VSMCs only migrated for a very limited distance too. By contrast, the

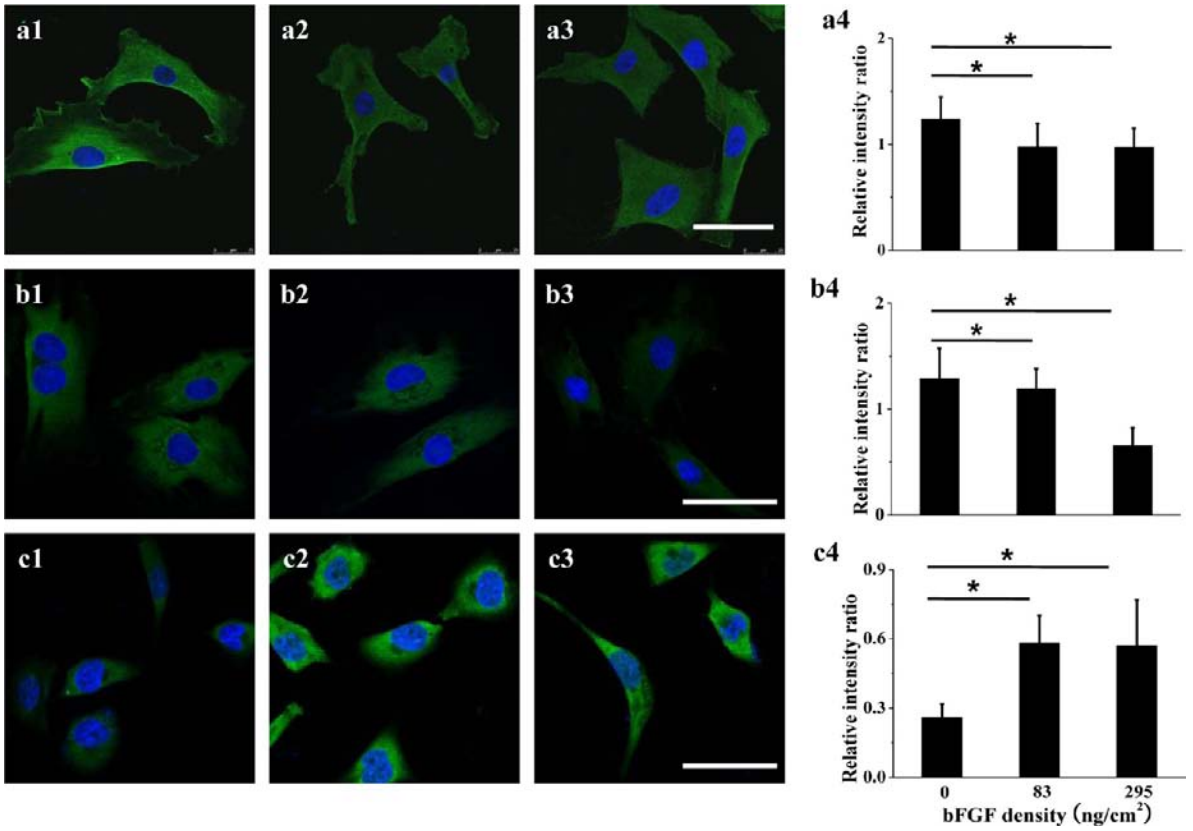

Figure 8. CLSM images of RhoA in (a) VSMCs, (b) MSCs, and (c) ECs cultured for 24 h on surfaces of bFGF with a density of (1) 0 ng/cm^2, (2) 83 ng/cm^2, and (3) 295 ng/cm^2, respectively. RhoA and cell nucleus were stained by the monoclonal antibody (green) and DAPI (blue), respectively. The scale bar is 50 μm. (4) Fluorescence intensity ratio of RhoA calculated from (1) to (3) by IPP software as a function of bFGF density (relative to glass surface), respectively. * indicates significant difference at $p < 0.05$.

VSMCs traveled a longer distance on the surfaces with a moderate bFGF density (Figure 3b).

The average migration rates of VSMCs, ECs, and MSCs on different surfaces were summarized in Figure 4. The VSMCs, ECs, and MSCs have a comparable migration rate (5−8 μm/h) on the TMSPMA surface. The bFGF density has no significant influence on the mobility of MSCs and ECs, but influences the migration rate of VSMCs apparently.[40] The migration rate of VSMCs initially increased along with the increase of bFGF density and reached the highest value (21.5 μm/h) with a bFGF density of 83 ng/cm^2, and then slightly decreased and leveled off with still higher densities of bFGF (>130 ng/cm^2). By contrast, along with the increase of heparin density the cell migration rate was monotonously accelerated within a smaller extent (Figure S3), reflecting the weak effect of heparin molecules on cell migration.[41] All the results suggest that the bFGF density on the substrates dominates the cell mobility in a cell type and density-dependent manner.

Molecular Mechanism of Cell Mobility on bFGF Surfaces. It is well recognized that the cell motility can be controlled by the surface properties. For example, we found previously that the cell migration is dominated by the PEG grafting density on the surface due to the alternation of cell adhesion force.[9] In this study, the surface bFGF density can dominate the cell mobility in a cell type and density-dependent manner. However, the cell adhesion force of VSMCs was not significantly influenced by the surface bFGF density (Figure S1b), suggesting a more complicated mechanism comes into play.[42] In order to unveil the molecular mechanism that regulates the cell migration by the surface-tethered bFGF molecules and the intrinsic reason why different cells respond diversely to the bFGF density, the expression levels of several key signaling proteins of different cells as a function of surface bFGF density were analyzed (Figures 5−9).

bFGFR, the cell-surface receptor of bFGF, is able to bind with bFGF. It is activated and involved in multiple signal transduction processes, and regulates an extensive scale of cellular processes, including proliferation and migration.[43,44] The recognition and binding of bFGF by bFGFR is the earliest stage for cells to react to bFGF, and then triggers a series of downstream signaling pathways. It has been reported that FGFR activation on cells can promote the cell migration.[45−47] As shown in Figure 5, the expression level of bFGFR is significantly enhanced by the presence of bFGF molecules regardless of the cell type and bFGF surface density. Thus, conjugation of bFGF onto the substrate does contribute to the enhanced mobility of VSMCs. However, the enhanced expression of bFGFR (Figure 5b,c), which suggests greater interaction between bFGFR and bFGF in MSCs and ECs too, did not result in higher mobility. This might be attributed to the different signal transduction processes in different types of cells. Thus, the expression levels of several key intracellular migration-related proteins were further investigated.

Cdc42, Rac1, and RhoA are members of Rho family of guanosine triphosphatases (Rho-GTPase) that transduce extracellular signals from G-coupled protein receptors (GPCR), integrins, and growth factor receptors to modulate signaling pathways.[48] Cdc42 is a master regulator of cell polarity in

dx.doi.org/10.1021/bc300670t | Bioconjugate Chem. 2013, 24, 1302−1313

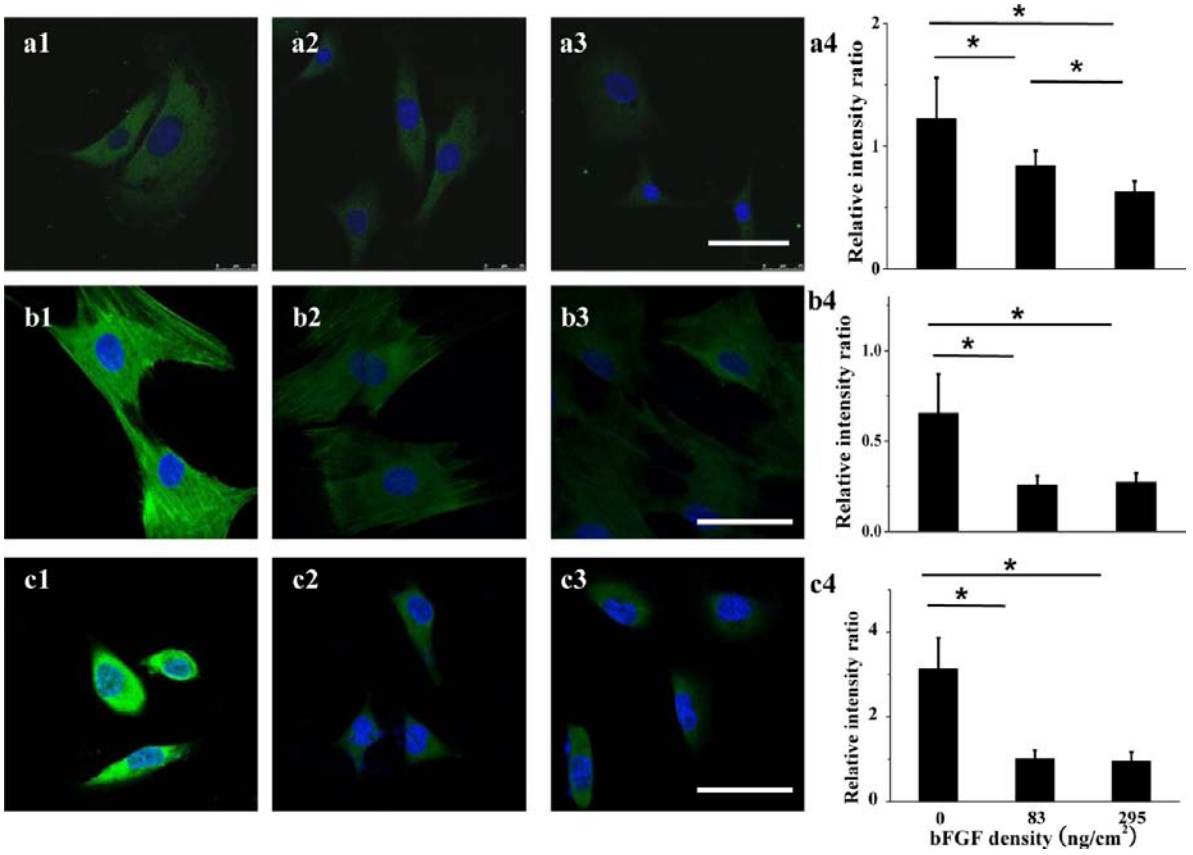

Figure 9. CLSM images of myosin IIA in (a) VSMCs, (b) MSCs, and (c) ECs cultured for 24 h on surfaces of bFGF with a density of (1) 0 ng/cm^2, (2) 83 ng/cm^2, and (3) 295 ng/cm^2, respectively. myosin IIA and cell nucleus were stained by the monoclonal antibody (green) and DAPI (blue), respectively. The scale bar is 50 μm. (4) Fluorescence intensity ratio of myosin IIA calculated from (1) to (3) by IPP software as a function of bFGF density (relative to glass surface). * indicates significant difference at $p < 0.05$.

eukaryotic organisms ranging from yeast to humans, which is the prerequisite of cell migration.[49] Rac1 is a member of the Rac subfamily, which regulates the cytoskeletal remodeling and membrane ruffling.[50] RhoA plays an important role during the formation of focal adhesion and the generation of contraction.[51] Both Rac1 and RhoA are involved in cell dynamic locomotion process. Myosins comprise a family of adenosine triphosphate (ATP)-dependent motor proteins, and are best known for their role in muscle contraction and their involvement in a wide range of other eukaryotic motility processes. Myosin IIA is a member of the subfamily responsible for producing contraction force from the interaction with actin filaments.[52]

Herein these four migration-related proteins secreted by cells on different surfaces were investigated by immunofluorescence staining (Figures 6−9) and the relative fluorescence intensity was quantified. The cellular expression of Cdc42 (Figure 6a) and Rac1 (Figure 7a) of the VSMCs was significantly enhanced, and that of RhoA and myosin IIA was significantly reduced on the bFGF surfaces. These proteins control signal transduction pathways by recurrently switching from a guanosine diphosphate (GDP)-bound form to a guanosine triphosphate (GTP)-bound form.[53] Once activated, they interact with cellular target proteins to generate multiple complex downstream responses (Figure 10).[54] Briefly, the Rac activation stimulates phosphatidylinositol 3-kinase (PI 3-kinase) and leads to the production of phosphatidylinositol-(3,4,5)-triphosphate ($PI(3,4,5)P_3$), which is required for cell chemotaxis and actin polymerization at the front.[55] The specific activation of partitioning-defective 6 (Par6) and protein kinase Cζ (PKCζ) by Cdc42 at cell leading edge is essential for establishing polarization and determining cell direction.[56] Besides, the Ser/Thr kinase p65PAK is also activated upon either Rac or Cdc42 activation which is important in regulating focal adhesion circular turnover.[57] Therefore, the increasing level of Rac and Cdc42 monotonically accelerates the cell migration. The decline of Rho function with the increase of bFGF density is attributed to the activated Rac.[58] Rho acts via Rho-associated kinases (ROCKs) and myosin regulatory light chain (MLC) which acts in concert to regulate cell contractility.[59−61] The effect of Rho on cell migration rate depends on the cell type.[62] For those adherent cells with high level of stress fibers, i.e., VSMCs, the Rho-induced attachment is suppressed by reducing Rho which turns out to accelerate cell migration.[63]

Myosin, usually in association with actin filament, is responsible for F-actin anterograde flow and retrograde flow in the lamella in the cell body.[64] It participates in activities like cellular contractility, focal adhesions, actin stress fiber organization, and tail retraction.[65] Sandquist et al. found that the absence of myosin IIA enhances the migration of cancer cells with high rate of wound closure, but suppresses the mobility of single cell.[66] Nevertheless, Ram et al. found that the myosin IIA-knockout cells exhibit 2−3-fold increase in mobility and display extensive ruffling structures.[67] Thus, myosin IIA has a biphasic effect on cell migration and this was proven in our finding. With the increase of surface-conjugated bFGF density, myosin IIA was suppressed and the cell migration rate increased. But on

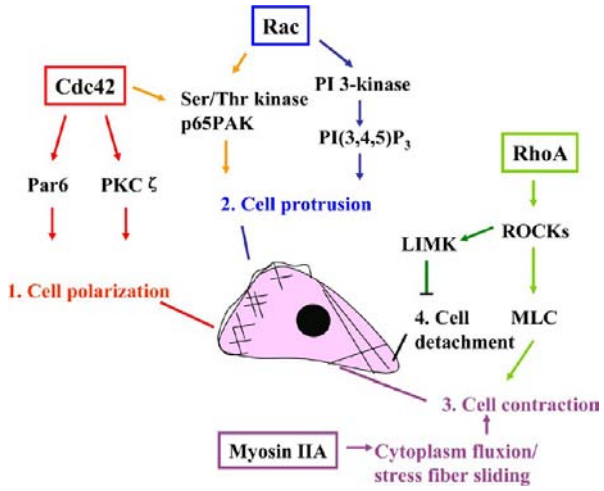

Figure 10. Schematic illustration of cellular signaling pathways of migration-related proteins that control the cell migration. Rac activation stimulates actin polymerization at the front. Cdc42 is essential for establishing polarization and Rac is important in regulating focal adhesion circular turnover. Therefore, the increasing level of Rac and Cdc42 accelerates monotonically the cell migration. The decline of Rho function with the increase of bFGF density is attributed to the activated Rac. For those adherent cells with high level of stress fibers, i.e., VSMCs, the Rho-induced attachment suppresses cell migration.

the surface with high density of bFGF, the cell migration was significantly decreased with further reduced myosin IIA.

Thus, the VSMCs have the lowest mobility on the TMSPMA surface due to the high expression of RhoA, which blocks the dissociation of cell adhesion, and low expression of Cdc42 and Rac1, which are able to induce cell polarization and cytoskeleton remodeling. On the bFGF surfaces, the cells have higher mobility due to the lower expression of RhoA and higher expression of Cdc42 and Rac1. However, on the surfaces with the highest bFGF density (295 ng/cm^2) the expression of Myosin IIA which contributes to the contraction of cellular microfilament[50] was also decreased, leading to the slower cell migration. Governed by the interplay of all these migration-related proteins, the cells have the highest mobility on the surface with a medium bFGF density (83 ng/cm^2).

The MSCs showed enhanced expression of Cdc42 (Figure 6b) but reduced expression of RhoA (Figure 8b) and myosin IIA (Figure 9b) on the bFGF surfaces, which are favorable for cell migration. However, the expression level of Rac1 of the MSCs (Figure 7b) was reduced significantly on the bFGF surfaces, implying that the cell polarization is blocked. Taking all the factors into consideration, the mobility of the MSCs was not obviously enhanced on the bFGF surfaces. The expression level of Cdc 42 (Figure 6c) and Rac1 (Figure 7c) of the ECs was not significantly altered on the bFGF surfaces. However, the expression level of RhoA (Figure 8c) was enhanced and that of myosin IIA (Figure 9c) was reduced on the bFGF surfaces. These contradictory effects of bFGF result in the similar mobility of ECs on the different surfaces. All the results suggest that the diverse influence of bFGF surface on the cell migration is attributed to the different signaling pathways in different types of cells.

Although previous research also revealed the effect of chemoattractants such as epidermal growth factor (EGF), collagens (types II, III, and V), and laminin on cell migration,[41,68] no attempt has been made to disclose the mechanism on a molecular level. bFGF is a chemoattractant and motigen which mediates a variety of signaling pathways in different types of cells.[69] It is suggested that cells are not able to sense the spatial rise and fall of high enough concentration of bFGF, leading to reduction of cell mobility.[70,71] Our results confirm that the migration of different types of cells is mainly governed by the synergistic effect of the migration-related signals rather than the adhesion force in a cell-type dependent manner.

CONCLUSION

The study of cell migration behaviors on surfaces with different density of growth factors is of paramount importance because it can disclose many physiological and pathological events, and eventually guide the design of biomaterials with better performance in tissue regeneration. In this work, the bFGF molecules of different density were successfully prepared by bioconjugation technology. The bFGF density dominated the mobility of VSMCs but had no significant influence on that of ECs and MSCs. The migration rate of VSMCs increased initially along with the increase of bFGF density and reached the maximum value (~22 μm/h) at a moderate density (83 ng/cm^2), and then decreased when the bFGF density further increased.

Immunofluorescent staining was used to study the bFGFR and migration-related proteins of the different types of cells. The expression of bFGFR in all types of cells was significantly enhanced on the bFGF surfaces. For VSMCs, the expression of Cdc42 and Rac1 was upregulated significantly and that of RhoA and Myosin IIA was downregulated significantly on the surfaces with a moderate bFGF density, which explains the fastest cell mobility. By contrast, although a part of migration-related proteins in the MSCs and the ECs were also activated on the bFGF surfaces, the downregulation of Rac1 expression in the MSCs and the upregulation of RhoA expression in the ECs are not favorable for cell migration, leading to the slower mobility of these two types of cells compared with the VSMCs.

In summary, the present strategy of bFGF gradient preparation is proven to be chemically simple under mild conditions. The surface density of heparin and bFGF can be easily tuned. Moreover, the two step strategy avoids the direct chemical reaction with vulnerable bFGF and thereby maximally maintains the bioactivity of tethered bFGF. It is demonstrated that the density of surface-conjugated bFGF molecules plays a primary role on migration of VSMCs, but has no effect on the MSCs and ECs. This surface immobilization strategy also provides a useful approach to enhance the understanding of bFGF-induced cell migration at a fundamental level, providing design criteria for advanced biomaterials for regenerative medicine.

ASSOCIATED CONTENT

Supporting Information

Cell number and adhesion force of VSMCs on bFGF surfaces. This material is available free of charge via the Internet at http://pubs.acs.org.

AUTHOR INFORMATION

Corresponding Author

*E-mail: cygao@mail.hz.zj.cn. Fax: +86-571-87951108.

Notes

The authors declare no competing financial interest.

■ ACKNOWLEDGMENTS

This study is financially supported by the Natural Science Foundation of China (20934003), and the Major State Basic Research Program of China (2011CB606203). Z.W. Mao thanks Young Teacher Programs Foundation of Ministry of Education of China (20100101120034), and "Qianjiang" outstanding researcher funding of Zhejiang Province (J20110541).

■ REFERENCES

(1) Kim, B., Park, I., Hoshiba, T., Jiang, H., Choi, Y., Akaike, T., and Cho, C. S. (2011) Design of artificial extracellular matrices for tissue engineering. *Prog. Polym. Sci. 36*, 238−268.
(2) Mantovani, D. (2007) Macromolecular biomaterials interfacing with cells. *Macromol. Biosci. 7*, 541−543.
(3) Anselme, K. (2011) Biomaterials and interface with bone. *Osteoporos. Int. 22*, 2037−2042.
(4) Wei, Y., Ji, Y., Xiao, L., Lin, Q., and Ji, J. (2011) Different complex surfaces of polyethyleneglycol (PEG) and REDV ligand to enhance the endothelial cells selectivity over smooth muscle cells. *Colloids Surf., B: Biointerfaces 84*, 369−378.
(5) Barheine, S., Hayakawa, S., Osaka, A., and Jaeger, C. (2009) Surface, interface, and bulk structure of borate containing apatitic biomaterials. *Chem. Mater. 21*, 3102−3109.
(6) Godwin, J. W., and Brockes, J. P. (2006) Regeneration, tissue injury and the immune response. *J. Anat. 209*, 423−432.
(7) Martin, P. (1997) Wound healing-aiming for perfect skin regeneration. *Science 276*, 75−81.
(8) Bernstein, L. R., and Liotta, L. A. (1994) Molecular mediators of interactions with extracellular matrix components in metastasis and angiogenesis. *Curr. Opin. Oncol. 6*, 106−113.
(9) Wu, J. D., Mao, Z. W., and Gao, C. Y. (2012) Controlling the migration behaviors of vascular smooth muscle cells by methoxy poly(ethylene glycol) brushes of different molecular weight and density. *Biomaterials 33*, 810−820.
(10) Mann, B. K., and West, J. L. (2002) Cell adhesion peptides alter smooth muscle cell adhesion, proliferation, migration, and matrix protein synthesis on modified surfaces and in polymer scaffolds. *J. Biomed. Mater. Res. 60*, 86−93.
(11) Guarnieri, D., de Capua, A., Ventre, M., Borzacchiello, A., Pedone, C., Marasco, D., Ruvo, M., and Netti, P. A. (2010) Covalently immobilized RGD gradient on PEG hydrogel scaffold influences cell migration parameters. *Acta Biomater. 6*, 2532−2539.
(12) Wacker, B. K, Alford, S. K., Scott, E. A., Das, T. M., Longmore, G. D., and Elbert, D. L. (2008) Endothelial cell migration on RGD-peptide-containing PEG hydrogels in the presence of sphingosine 1-phosphate. *Biophys. J. 94*, 273−285.
(13) Dalton, B. A., McFarland, C. D., Gengenbach, T. R., Griesser, H. J., and Steele, J. G. (1998) Polymer surface chemistry and bone cell migration. *J. Biomater. Sci. Polym. Ed. 9*, 781−799.
(14) Smith, J. T., Tomfohr, J. K., Wells, M. C., Beebe, T. J., Kepler, T. B., and Reichert, W. M. (2004) Measurement of cell migration on surface-bound fibronectin gradients. *Langmuir 20*, 8279−8286.
(15) Smith, J. T., Elkin, J. T., and Reichert, W. M. (2006) Directed cell migration on fibronectin gradients: effect of gradient slope. *Exp. Cell. Res. 312*, 2424−2432.
(16) Cai, K. Y., Kong, T. T., Wang, L., Liu, P., Yang, W. H., and Chen, C. (2010) Regulation of endothelial cells migration on poly(D, L-lactic acid) films immobilized with collagen gradients. *Colloids Surf., B: Biointerfaces 79*, 291−297.
(17) Szabo, S., and Sandor, Z. (1996) Basic fibroblast growth factor and PDGF in GI diseases. *Baillieres Clin. Gastroenterol. 10*, 97−112.
(18) Bartlett, P. F., Brooker, G. J., Faux, C. H., Dutton, R., Murphy, M., Turnley, A., and Kilpatrick, T. J. (1998) Regulation of neural stem cell differentiation in the forebrain. *Immunol. Cell Biol. 76*, 414−418.
(19) Rosengart, T. K., Budenbender, K. T., Duenas, M., Mack, C. A., Zhang, Q. X., and Isom, O. W. (1997) Therapeutic angiogenesis: a comparative study of the angiogenic potential of acidic fibroblast growth factor and heparin. *J. Vasc. Surg. 26*, 302−312.
(20) Yoneda, A., Asada, M., Oda, Y., Suzuki, M., and Imamura, T. (2000) Engineering of an FGF-proteoglycan fusion protein with heparin-independent, mitogenic activity. *Nat. Biotechnol. 18*, 641−644.
(21) Kawai, K., Suzuki, S., Tabata, Y., Ikada, Y., and Nishimura, Y. (2000) Accelerated tissue regeneration through incorporation of basic fibroblast growth factor-impregnated gelatin microspheres into artificial dermis. *Biomaterials 21*, 489−499.
(22) Katsuno, A., Aimoto, T., Uchida, E., Tabata, Y., Miyamoto, M., and Tajiri, T. (2011) The controlled release of basic fibroblast growth factor promotes a rapid healing of pancreaticojejunal anastomosis with potent angiogenesis and accelerates apoptosis in granulation tissue. *J. Surg. Res. 167*, 166−172.
(23) Stefonek-Puccinelli, T. J., and Masters, K. S. (2008) Co-immobilization of gradient-patterned growth factors for directed cell migration. *Ann. Biomed. Eng. 36*, 2121−2133.
(24) DeLong, S. A., Moon, J. J., and West, J. L. (2005) Covalently immobilized gradients of bFGF on hydrogel scaffolds for directed cell migration. *Biomaterials 26*, 3227−3234.
(25) Liu, L. Y., Ratner, B. D., Sage, E. H., and Jiang, S. Y. (2007) Endothelial cell migration on surface-density gradients of fibronectin, VEGF, or both proteins. *Langmuir 23*, 11168−11173.
(26) Sakakibara, Y., Tambara, K., Sakaguchi, G., Lu, F., Yamamoto, M., Nishimura, K., Tabata, Y., and Komeda, M. (2003) Toward surgical angiogenesis using slow-released basic fibroblast growth factor. Eur. *J. Cardiothoracic Surg. 24*, 105−111.
(27) Wissink, M. J., Beernink, R., Pieper, J. S., Poot, A. A., Engbers, G. H., Beugeling, T., van Aken, W. G., and Feijen, J. (2001) Binding and release of basic fibroblast growth factor from heparinized collagen matrices. *Biomaterials 22*, 2291−2299.
(28) Mao, Z. W., Ma, L., Zhou, J., Gao, C. Y., and Shen, J. C. (2005) Bioactive thin film of acidic fibroblast growth factor fabricated by layer-by-layer assembly. *Bioconjugate Chem. 16*, 1316−1322.
(29) Li, D., Ye, C., Zhu, Y., Qi, Y. Y., Gou, Z. R., and Gao, C. Y. (2011) Fabrication of poly(lactide-co-glycolide) scaffold embedded spatially with hydroxyapatite particles on pore walls for bone tissue engineering. *Polym. Adv. Technol. 23*, 1446−1453.
(30) Faham, S., Linhardt, R. J., and Rees, D. C. (1998) Diversity does make a difference: fibroblast growth factor-heparin interactions. *Curr. Opin. Struct. Biol. 8*, 578−586.
(31) Ornitz, D. M. (2000) FGFs, heparan sulfate and FGFRs: complex interactions essential for development. *Bioessays 22*, 108−112.
(32) Lam, K., Rao, V. S., and Qasba, P. K. (1998) Molecular modeling studies on binding of bFGF to heparin and its receptor FGFR1. *J. Biomol. Struct. Dyn. 15*, 1009−1027.
(33) Gospodarowicz, D., and Cheng, J. (1986) Heparin protects basic and acidic FGF from inactivation. *J. Cell. Physiol. 128*, 475−484.
(34) Kajio, T., Kawahara, K., and Kato, K. (1992) Stabilization of basic fibroblast growth factor with dextran sulfate. *Febs Lett. 306*, 243−246.
(35) Marui, A., Kanematsu, A., Yamahara, K., Doi, K., Kushibiki, T., Yamamoto, M., Itoh, H., Ikeda, T., Tabata, Y., and Komeda, M. (2005) Simultaneous application of basic fibroblast growth factor and hepatocyte growth factor to enhance the blood vessels formation. *J. Vasc. Surg. 41*, 82−90.
(36) Qu, D., Li, J., Li, Y., Gao, Y., Zuo, Y., Hsu, Y., and Hu, J. (2011) Angiogenesis and osteogenesis enhanced by bFGF ex vivo gene therapy for bone tissue engineering in reconstruction of calvarial defects. *J. Biomed. Mater. Res. A 96*, 543−551.
(37) Yang, Y., Xia, T., Zhi, W., Wei, L., Weng, J., Zhang, C., and Li, X. H. (2011) Promotion of skin regeneration in diabetic rats by electrospun core-sheath fibers loaded with basic fibroblast growth factor. *Biomaterials 32*, 4243−4254.
(38) Heydarkhan-Hagvall, S., Helenius, G., Johansson, B. R., Li, J. Y., Mattsson, E., and Risberg, B. (2003) Co-culture of endothelial cells and smooth muscle cells affects gene expression of angiogenic factors. *J. Cell Biochem. 89*, 1250−1259.
(39) Kasper, G., Dankert, N., Tuischer, J., Hoeft, M., Gaber, T., Glaeser, J. D., Zander, D., Tschirschmann, M., Thompson, M., Matziolis, G., and Duda, G. N. (2007) Mesenchymal stem cells

regulate angiogenesis according to their mechanical environment. *Stem Cells 25*, 903−910.
(40) Bos, G. W., Scharenborg, N. M., Poot, A. A., Engbers, G. H., Beugeling, T., van Aken, W. G., and Feijen, J. (1999) Proliferation of endothelial cells on surface-immobilized albumin-heparin conjugate loaded with basic fibroblast growth factor. *J. Biomed. Mater. Res. 44*, 330−340.
(41) Terranova, V. P., DiFlorio, R., Lyall, R. M., Hic, S., Friesel, R., and Maciag, T. (1985) Human endothelial cells are chemotactic to endothelial cell growth factor and heparin. *J. Cell Biol. 101*, 2330−2334.
(42) Lindner, V., Lappi, D. A., Baird, A., Majack, R. A., and Reidy, M. A. (1991) Role of basic fibroblast growth factor in vascular lesion formation. *Circ. Res. 68*, 106−113.
(43) Acevedo, V. D., Ittmann, M., and Spencer, D. M. (2009) Paths of FGFR-driven tumorigenesis. *Cell Cycle 8*, 580−588.
(44) Kadam, S., McMahon, A., Tzou, P., and Stathopoulos, A. (2009) FGF ligands in Drosophila have distinct activities required to support cell migration and differentiation. *Development 136*, 739−747.
(45) Li, J., Dai, G., Cheng, Y. B., Qi, X., and Geng, M. Y. (2011) Polysialylation promotes neural cell adhesion molecule-mediated cell migration in a fibroblast growth factor receptor-dependent manner, but independent of adhesion capability. *Glycobiology 21*, 1010−1018.
(46) Ishiwata, T., Matsuda, Y., Yamamoto, T., Uchida, E., Korc, M., and Naito, Z. (2012) Enhanced expression of fibroblast growth factor receptor 2 IIIc promotes human pancreatic cancer cell proliferation. *Am. J. Pathol. 180*, 1928−1941.
(47) Nomura, S., Yoshitomi, H., Takano, S., Shida, T., Kobayashi, S., Ohtsuka, M., Kimura, F., Shimizu, H., Yoshidome, H., Kato, A., and Miyazaki, M. (2008) FGF10/FGFR2 signal induces cell migration and invasion in pancreatic cancer. *Br. J. Cancer 99*, 305−313.
(48) Etienne-Manneville, S., and Hall, A. (2002) Rho GTPases in cell biology. *Nature 420*, 629−635.
(49) Itoh, R. E., Kurokawa, K., Ohba, Y., Yoshizaki, H., Mochizuki, N., and Matsuda, M. (2002) Activation of rac and cdc42 video imaged by fluorescent resonance energy transfer-based single-molecule probes in the membrane of living cells. *Mol. Cell. Biol. 22*, 6582−6591.
(50) Ryu, Y., Takuwa, N., Sugimoto, N., Sakurada, S., Usui, S., Okamoto, H., Matsui, O., and Takuwa, Y. (2002) Sphingosine-1-phosphate, a platelet-derived lysophospholipid mediator, negatively regulates cellular Rac activity and cell migration in vascular smooth muscle cells. *Circ. Res. 90*, 325−332.
(51) van Nieuw, A. G., Koolwijk, P., Versteilen, A., and van Hinsbergh, V. W. (2003) Involvement of RhoA/Rho kinase signaling in VEGF-induced endothelial cell migration and angiogenesis in vitro. *Arterioscler. Thromb. Vasc. Biol. 23*, 211−217.
(52) Ridley, A. J., Schwartz, M. A., Burridge, K., Firtel, R. A., Ginsberg, M. H., Borisy, G., Parsons, J. T., and Horwitz, A. R. (2003) Cell migration: integrating signals from front to back. *Science 302*, 1704−1709.
(53) Raftopoulou, M., and Hall, A. (2004) Cell migration: Rho GTPases lead the way. *Dev. Biol. 265*, 23−32.
(54) Bishop, A. L., and Hall, A. (2000) Rho GTPases and their effector proteins. *Biochem. J. 348*, 241−255.
(55) Stephens, L., Ellson, C., and Hawkins, P. (2002) Roles of PI3Ks in leukocyte chemotaxis and phagocytosis. *Curr. Opin. Cell Biol. 14*, 203−213.
(56) Etienne-Manneville, S., and Hall, A. (2003) Cdc42 regulates GSK-3beta and adenomatous polyposis coli to control cell polarity. *Nature 421*, 753−756.
(57) Manabe, R., Kovalenko, M., Webb, D. J., and Horwitz, A. R. (2002) GIT1 functions in a motile, multi-molecular signaling complex that regulates protrusive activity and cell migration. *J. Cell. Sci. 115*, 1497−1510.
(58) Sanders, L. C., Matsumura, F., Bokoch, G. M., and de Lanerolle, P. (1999) Inhibition of myosin light chain kinase by p21-activated kinase. *Science 283*, 2083−2085.
(59) Alblas, J., Ulfman, L., Hordijk, P., and Koenderman, L. (2001) Activation of Rhoa and ROCK are essential for detachment of migrating leukocytes. *Mol. Biol. Cell 12*, 2137−2145.
(60) Kawano, Y., Fukata, Y., Oshiro, N., Amano, M., Nakamura, T., Ito, M., Matsumura, F., Inagaki, M., and Kaibuchi, K. (1999) Phosphorylation of myosin-binding subunit (MBS) of myosin phosphatase by Rho-kinase in vivo. *J. Cell Biol. 147*, 1023−1038.
(61) Mitchison, T. J., and Cramer, L. P. (1996) Actin-based cell motility and cell locomotion. *Cell 84*, 371−379.
(62) Ridley, A. J. (2001) Rho GTPases and cell migration. *J. Cell Sci. 114*, 2713−2722.
(63) Cox, E. A., Sastry, S. K., and Huttenlocher, A. (2001) Integrin-mediated adhesion regulates cell polarity and membrane protrusion through the Rho family of GTPases. *Mol. Biol. Cell 12*, 265−277.
(64) Gupton, S. L., Anderson, K. L., Kole, T. P., Fischer, R. S., Ponti, A., Hitchcock-DeGregori, S. E., Danuser, G., Fowler, V. M., Wirtz, D., Hanein, D., and Waterman-Storer, C. M. (2005) Cell migration without a lamellipodium: translation of actin dynamics into cell movement mediated by tropomyosin. *J. Cell Biol. 168*, 619−631.
(65) Doyle, A. D., Kutys, M. L., Conti, M. A., Matsumoto, K., Adelstein, R. S., and Yamada, K. M. (2012) Microenvironmental control of cell migration: Myosin IIA is required for efficient migration in fibrillar environments through control of cell adhesion dynamics. *J. Cell Sci. 125*, 2244−2256.
(66) Sandquist, J. C., Swenson, K. I., Demali, K. A., Burridge, K., and Means, A. R. (2006) Rho kinase differentially regulates phosphorylation of nonmuscle myosin II isoforms A and B during cell rounding and migration. *J. Biol. Chem. 281*, 35873−35883.
(67) Even-Ram, S., Doyle, A. D., Conti, M. A., Matsumoto, K., Adelstein, R. S., and Yamada, K. M. (2007) Myosin IIA regulates cell motility and actomyosin-microtubule crosstalk. *Nat. Cell Biol. 9*, 299−309.
(68) Gunawan, R. C., Silvestre, J., Gaskins, H. R., Kenis, P. J., and Leckband, D. E. (2006) Cell migration and polarity on microfabricated gradients of extracellular matrix proteins. *Langmuir 22*, 4250−4258.
(69) Yamada, K. M., and Even-Ram, S. (2002) Integrin regulation of growth factor receptors. *Nat. Cell Biol. 4*, 75−76.
(70) Yoshida, A., Anand-Apte, B., and Zetter, B. R. (1996) Differential endothelial migration and proliferation to basic fibroblast growth factor and vascular endothelial growth factor. *Growth Factors 13*, 57−64.
(71) Seppa, H., Grotendorst, G., Seppa, S., Schiffmann, E., and Martin, G. R. (1982) Platelet-derived growth factor in chemotactic for fibroblasts. *J. Cell Biol. 92*, 584−588.